

# Computed Chaos or Numerical Errors

Lun-Shin Yao

Department of Mechanical and Aerospace Engineering

Arizona State University

Tempe, Arizona

E-mail: ls\_yao@asu.edu

## Abstract

Discrete numerical methods with finite time steps represent a practical technique to solve non-linear differential equations. This is particularly true for chaos since no analytical chaotic solution is known today. Using the Lorenz equations as an example it is demonstrated that computed results and their associated statistical properties are time-step dependent. There are two reasons for this behavior. First, it is well known that chaotic differential equations are unstable, and that any small error can be amplified exponentially near an unstable manifold. The more serious and less-known reason is that stable and unstable manifolds of singular points associated with differential equations can form virtual separatrices. The existence of a virtual separatrix presents the possibility of a computed trajectory actually jumping through it due to the finite time-steps of discrete numerical methods. Such behavior violates the uniqueness theory of differential equations and amplifies the numerical errors *explosively*. These reasons ensure that, even if the computed results are bounded; their independence of time-step should be established before accepting them as useful numerical approximations to the true solution of the differential equations. Due to the explosive amplification of numerical errors, no computed chaotic solution of differential equations that is independent of integration-time step has been found.

## 1. Introduction

In spite of numerous attempts, a convincing proof of the existence of the geometric Lorenz attractor for the Lorenz's differential equations was not achieved until recently. Tucker (2002) provided a solution to this problem, which is the 14th of the 18 challenging mathematical problems defined by Smale (1998). Viana (2000), in a review of the historical advancement of structural stability theories, explained the difficulties that Tucker had to overcome to complete his proof. The next step in the progression of this important research topic is the construction of the existing solution.

A possible approach to this issue is direct numerical integration, which is a powerful, popular, and convenient tool for solving initial-value problems for nonlinear differential equations arising in science and engineering. The use of such tools introduces truncation and rounding errors that often have a major impact on the quality of “computed results,” which are the product of an application of a certain algorithm in a certain computing environment. In some cases, these “computed results” may not provide a reasonable approximate solution to the original initial-value problem in any sense. In this paper these ideas are studied for a particular chaotic system based on the well-known Lorenz equations for variables  $x(t)$ ,  $y(t)$ , and  $z(t)$ . It is demonstrated that the numerical integration of this chaotic system is extremely sensitive to the integration time-step “near” the  $z$ -axis where stable and unstable manifolds intersect. Coupled with this behavior is the fact that different integration time-steps yield both “computed results” and computed statistical properties of the associated attractors that are dramatically different among them. These statistical properties can often be associated with physical quantities of interest in applications from science and engineering. Any “computed results” whose statistical properties are sensitive to integration time-steps are not useful approximations.

The sensitivity of “computed results” to integration time-steps has been identified for the Rössler equations (Stuart & Humphries, 1996, pp. 532-533). Rössler himself noted, in the fall of 1975, (Rössler 2000, p. 213) the important role-played by integration time-steps in his system. However, there was no attempt to connect this sensitivity to the statistical properties of the “similar” attractors shown in Figure 7.1 of Stuart & Humphries (1996),

and no explanations for these observations were provided. The sensitivity of “computed results” to integration time-steps has also been studied for the one-dimensional Kuramoto-Sivashinsky equation, a non-linear partial differential equation (Yao 2002).

The sensitivity to initial conditions has been studied for hyperbolic systems (Bowen 1975) and is an active topic for nearly hyperbolic systems (Dawson, Grebogi, Sauer, & Yorke 1994; Viana 2000; Palis 2000; Morales, Pacifico & Pujals 2002). In particular, the methods of shadowing for hyperbolic systems have shown that trajectories may be *locally* sensitive to initial conditions while being *globally* insensitive since true trajectories with adjusted initial conditions exist. Such trajectories are called shadowing trajectories, and lie very close to the long-time computed trajectories. However, systems of differential equations arising from physical applications are not hyperbolic. If the attractor is *transitive* (ergodic), all trajectories are inside the attractor so they are generally believed to be solutions of the underlying differential equations whatever the initial conditions are. Little is known about systems, which are not transitive (non-ergodic). Do & Lai (2004) have provided with a comprehensive review of previous work, and discussed the fundamental dynamical process that a long-time shadowing of non-hyperbolic systems is not possible. On the other hand, sensitivity to integration time-steps, the topic of the present work, leads to multiple attractors; consequently, *ad hoc* arguments based on the existence of a single attractor are not sufficient.

In the next section, we show that “computed results” as well as a corresponding long-time averaged statistical correlation display a sensitive dependence on integration time-steps. A systematic decrease in the magnitude of the time steps does not lead to a convergent pattern; rather irregularly fluctuating results are noted. Differences between different samples can be small in a suitable sense, but never demonstrate convergence, indicating that the bounded “computed results” are contaminated by numerical errors.

The third section contains a demonstration of the exponential amplification of a small difference between two trajectories, which involve different integration time-steps, which occurs when they move in the direction of an unstable manifold (the x-axis for the specific cases treated here). When two different, as just mentioned, trajectories move in

the direction of a stable manifold, their difference becomes smaller. This difference depends on the initial error introduced by the different time-steps.

In the fourth section, we show that a significant amplification of numerical errors occurs when a trajectory, in violation of theoretical expectations, jumps through a two-dimensional virtual separatrix. In contrast to the behavior noted in section 3, this behavior is independent of the differences induced by the integration time-steps before amplification.

Section 5 shows that “computed results” can be used to construct a strange attractor, even though they are time-step dependent. The computed trajectory seems to visit the edges of the attractor less frequently. This observation agrees with the finding by Tucker (2002) that the stretching rate near the edge of the attractor is smaller than  $\sqrt{2}$ , the required minimum value to ensure its transitivity (Viana 2000). Conclusions are discussed in the final section.

## 2. Time-Step Sensitive Numerical Solutions

We use the Lorenz equations,

$$\begin{aligned}\dot{x} &= -sx + sy, \\ \dot{y} &= rx - y - xz, \\ \dot{z} &= -bz + xy,\end{aligned}\tag{1}$$

with the widely used values of the parameters,  $s = 10$ ,  $r = 28$ ,  $b = 8/3$ , as the basis for showing that the “computed results” are time-step dependent and do not converge for large time. The initial conditions are  $x = 1$ ,  $y = -1$ ,  $z = 10$ . All results presented are generated by an explicit second-order accurate Adams-Bashforth method. The time history of  $x$  is plotted in Figure 1 for three different time steps, clearly showing the divergence of the “computed results.” Similar behavior was noted when Adams-Bashforth methods up to the fifth order; an implicit Crank-Nicholson method; second-order and forth-order Runge-Kutta method; adaptive methods as well as compact time-difference schemes. In no case was a convergent solution obtained for  $t \geq 20$ .

The trajectory for one of the cases of Figure 1 ( $\Delta t = 0.0001$ ) is shown in three projections in Figure 2 for the first 300,000 computational time steps. This figure is useful as a geometric aid to identifying the location (and reasons) for the observed divergence. Initially, the trajectory moves smoothly around the two singular points (reverse spiral), and from one singular point to the other. However, at a certain time identified by an arrow in the figure, the computed trajectory diverged. This behavior signals the “break-down” of the computation; it will be discussed in greater detail in Section 4.

The apparent random behavior in Figure 1 is consistent with the common expectation that it is impossible to repeat the time histories of chaotic different equations due to their extreme sensitivity. On the other hand, in order to be useful in scientific or engineering applications, the statistical properties of a chaotic “computed result,” which can be of physical significance, must *not* be sensitive to the integration time-step. As an example, Figure 3 displays the time-averaged  $L_2$  norms corresponding to the “computed results” of Figure 1,

$$E(t) = \frac{1}{t} \int_0^t |x^2| dt .$$

They also strongly depend on the integration time-step. Computations for much longer times than the ones shown in the figure reveal that the various  $E(t)$  continue to be dependent on the integration time-step and do not converge. For long time,  $E(t)$  can be interpreted as the moment of inertia of the numerical Lorenz attractor about  $x = 0$  since the attractor is assumed topologically transitive. Since  $E(t)$  is an important statistical and geometric property of the attractor, different  $E(t)$  implies different attractors. The geometric properties of the “computed results” will be examined in the next section to show that the sensitivity to integration time-steps is the consequence of repeated amplification of numerical errors.

### 3. Exponential Growth of Numerical Errors

The following discussion is based on the normal form of the Lorenz system (Tucker 2002; Viana 2000). With  $s = 10$ ,  $b = 8/3$ , and  $r = 28$ , these equations are

$$\begin{aligned}
\dot{x} &= 11.8x - 0.29(x+y)z, \\
\dot{y} &= -22.8y + 0.29(x+y)z, \\
\dot{z} &= -2.67z + (x+y)(2.2x - 1.3y)
\end{aligned} \tag{2}$$

Their three equilibrium points are:  $(0, 0, 0)$  and  $(\pm 5.5929, \pm 2.8981, 26.8698)$ . The coefficients of the linear terms in (2) are eigenvalues and represent the growth rates of  $x$ ,  $y$ , and  $z$ , respectively. The non-linear terms lead to energy transfers among  $x$ ,  $y$  and  $z$  (Yao 1999). Far away from the three equilibrium points, the net effect is attracting since the sum of the eigenvalues is negative. Once a trajectory moves close to the three equilibrium points, it is trapped in a complex attractor due to the competition between attraction and repulsion of the three equilibrium points. This shows that the Lorenz attractor is inside a large attracting open set; hence, it is *robust* (Viana 2000).

The Euler method is used to numerically integrate the above equations. The initial conditions are the same as those used in Section 2. An explicit second-order-accurate Adams-Bashforth method was also used, and showed that the results are independent of these two numerical methods. These results, properly interpreted, identify two mechanisms that contribute to the sensitivity of the “computed results” to the integration time-step. The first of these mechanisms will be discussed in the following material, the second in Section 4.

The first mechanism is associated with the movement of the trajectory toward the  $z$ -axis (Figure 4). Equation (2) shows that, as the value of  $(x+y)$  becomes small, the value of the non-linear terms in the  $z$  equation decreases to near zero. This causes  $z$  to move exponentially toward  $z = 0$ , but the time required to reach  $z = 0$  is infinite.

Simultaneously, the value of  $x$  increases exponentially so that the trajectory turns sharply toward the direction of increasing  $x$  since the  $x$ -axis is the unstable manifold. In order to show the sensitivity to the integration time-steps, two different time steps, but the same initial conditions, were used to integrate equation. (2). The results show that the errors accumulated before the trajectory reaches the  $z$ -axis are amplified exponentially along the  $x$  direction and cause substantial numerical errors in the computation. It is clear that this amplification begins near the  $z$ -axis. The differences between the two trajectories for

different integration time-steps decreases as they approach the  $z$  axis (along the direction of the stable manifold), but start to increase exponentially as they turn toward the direction of the unstable manifold. This is a typical example for a positive Lyapunov exponent, and also is a hint about the existence of Smale's horseshoe. As the “computed results” repeatedly pass through the region just described, the corresponding trajectories move further apart. The study of whether such trajectories are shadowable for nearly hyperbolic systems is a current research topic. (Palis 2000; Morales, Pacifico & Pujals 2002; Tucker 2002). Even though it may be shadowable, its statistical properties cannot be determined (Dawson, Grebogi, Sauer & Yorke 1994).

#### 4. Explosive Amplification of Numerical Errors

The second mechanism occurs close to the  $z$ -axis, where the trajectory can turn in two opposite directions depending on whether the trajectory arrives at positive or negative  $x$  (Figure 5) since the  $z$ -axis is the intersection of stable and unstable manifolds. This means that a small numerical error can be “explosively” amplified. The breakdown of the computed results presented in Figure 2 belongs to this class. The reason for this “unshadowable” amplification of numerical errors is explained below.

It will be demonstrated in Section 5 that the trajectory frequently visits the neighborhood of the  $z$ -axis ( $0 \leq z \leq 15$ ), where the values of  $x$  and  $y$  are small. It is clear from equation (2) that, if the trajectory starts on the  $z$ -axis, it will stay on it forever so that the  $z$ -axis is an invariant set for the saddle at the origin. A trajectory in the *inset* of a limit point will approach the limit point asymptotically. The inset of an attractor is called its basin. The separatrix is defined as the complement of the basins of attraction. The initial state of a trajectory must belong to a separatrix if its future ( $\omega$ ) limit set is not an attractor.

Therefore, a separatrix consists of the insets of the non-attractive (or exceptional) limit sets. An *actual* separatrix separates basins. However, if it does not actually separate basins, it is called a *virtual* separatrix (Abraham & Shaw 1992). A computed trajectory cannot jump through a separatrix since that would violate the uniqueness theorem. Thus, a computed trajectory that does, in fact, jump through a separatrix means that the “computed results” violate the differential equations.

The following linearized analysis shows that the inset of the saddle point at the origin near the z-axis is a two-dimensional surface that includes the z-axis. This inset is a virtual separatrix embedded in the attractor. The linearized equations (2), near z-axis to the first order, are

$$\begin{aligned}\dot{x} &= 11.8x - 0.29(x + y)z, \\ \dot{y} &= -22.8y + 0.29(x + y)z, \\ \dot{z} &= -2.67z\end{aligned}\tag{3}$$

The solution for z is simply

$$z = z_0 e^{-2.67t},\tag{4}$$

where  $0 \leq z_0 \leq 15$  is the initial z location inside the attractor. The trajectories that reach the z-axis are found by setting

$$\begin{aligned}x &= h(y, z) = A(z)y + O(y^2), \\ h(0, z) &= 0,\end{aligned}\tag{5}$$

where  $A(z)$  is a function to be determined. Equation (5) defines the local stable and unstable manifolds near the z-axis. Using equations (5), the first two of equations (3) become

$$\begin{aligned}\dot{x} &= \frac{dh}{dy} \dot{y} \\ &= \frac{dh}{dy} [-22.8y + 0.29(h + y)z] \\ &= 11.8h - 0.29(h + y)z.\end{aligned}\tag{6}$$

The h can be determined by solving (6) with (4). Comparison of the result with (5) provides



$$A = B \left[ 1 \pm (1 - B^{-2})^{1/2} \right],$$

$$B = \frac{59.66}{z} - 1, \tag{7}$$

where the minus sign is for trajectories approaching the z-axis (stable manifold), and the plus sign is for the trajectories leaving it (unstable manifold). This shows that the local stable manifold is a two-dimensional surface forming, with the z-axis, the inset of the saddle point at the origin. Moreover, this result shows that the local stable and unstable manifolds approach the y-axis and x-axis, respectively, as  $z$  decreases to zero. A trajectory approaching the z-axis along the stable manifold can only move away along one branch of the unstable manifold without jumping through the virtual separatrix. The computed trajectories in figures 3, 4, and 5 display this behavior.

It is clear that the stable and unstable manifolds act as virtual separatrices and roughly divide the x-y plane (*Poincare'* map) into four quadrants locally near the z-axis. All meaningful trajectories should only travel in the first and third quadrants, but a *computed* trajectory may mistakenly move into the second and fourth quadrants, two forbidden zones, after jumping through the stable manifolds because of numerical errors introduced by finite integration time-steps, as shown in Figures 5c and 6c. Such numerical errors substantially alter the shape of the attractor; this matter will be further discussed in the next section. Once a computed trajectory moves into a forbidden zone, it can return to its “proper” track only at the beginning of a period of “winding” away from one of the two fixed points above the origin and forming the “wing of a butterfly.” Dawson, Grebogi, Sauer & Yorke (1994) have pointed out that a continuous shadowing trajectory cannot exist for such a trajectory, that is, it is *unshadowable*.

The shortcoming of a discrete numerical method is that it cannot exactly reach a surface of zero thickness. It is obvious that one of the two computed trajectories, shown in Figures 5 and 6, has passed through the two-dimensional inset of the saddle point at the origin, thereby violating the uniqueness theorem. In Figure 6a and 6b, four slightly different integration time steps were used. The corresponding computed trajectories moved closer to the z-axis within a circle of radius  $10^{-10}$ . It is interesting to note that the

two computed trajectories (cases A and B) that did not jump through the virtual separatrix agree with each other, as do the two computed trajectories (cases C and D) that jump through the virtual separatrix and violate the differential equations. However, note that these two sets of computed trajectories are substantially different from each other.

## 5. Lorenz Attractor

The locations where numerical errors are amplified can be better discussed in terms of a Lorenz attractor. It should be emphasized that we do not have a method to explicitly compute the true Lorenz attractor due to unavoidable numerical errors. A computed Lorenz attractor for  $\Delta t = 10^{-5}$ , and the initial condition (1, -1, 10) is used for the following discussion. The computation is carried out for  $10^8$  time-steps, and recorded every 1,000 time-steps. The attractor is constructed using 100,000 points, admittedly insufficient, but there are limitations due to the speed of the available computer.

Thin slices of the computed attractor normal to the z-axis are plotted at four different z locations in Figure 7. A short curve above the attractor shows that the computed trajectory rapidly enters the attractor from its initial location. This is because the attractor is *robust*. The bottom of the attractor looks like a “thin sheet,” with the z-axis embedded in it, as shown in Figure 7a. For the purpose of demonstration, an expanded cartoon of the computed thin-attractor section of Figure 7a appears in Figure 9. It shows that the size of the attractor section contaminated by numerical errors is twice as large as the correct one, and its shape is also quite different. This suggests that effect of numerical errors is by no means small.

Moving to  $z = 17.9$ , the attractor starts to “split” near its center and the z-axis is no longer embedded in it, as shown in Figure 7b. Above this value of z, the linearized analysis of Section 4 is not valid. For even larger values of z, the attractor splits into two parts due to the attraction from the two equilibrium points. The two large dots in Figure 7c locate the equilibrium points that no computed trajectory can reach; hence, there are two “holes” in the computed attractor near the two equilibrium points. In Figures 7 and 8, it is clear

that the two-dimensional inset of the saddle at the origin connects the two-dimensional outsets of the other two fixed points.

Higher up, the cross-section of the computed attractor shrinks and finally disappears for  $z > 40$ . Thin slices of the computed attractor normal to the  $x$ -axis are plotted in Figure 8. For small  $x$ , the attractor splits into two symmetric parts, which look very much like a “butterfly,” as is well known, when viewed from other angles. The attractor is very thin due to the strong contraction of the Lorenz equations (Viana 2000; Tucker 2002).

A single simulation used to construct a numerical Lorenz attractor indicates that the orbit is *dense*, and the computed attractor is *transitive* and *indecomposable*. The plots, in Figures 7 and 8, show that the attractor is finite and closed; hence, it is *compact* and *invariant* for a given time step. The plot also shows that the computed trajectory visits the edge of the attractor less frequently than its interior, agreeing with Tucker’s theorem (Viana 2000; Tucker 2002). In addition, this trajectory is sensitive to the initial condition; therefore, it is a *strange* attractor (Viana 2000; Guckenheimer & Holmes 1983). However, recall that the computed attractor is also sensitive to integration time-steps: different time-steps result in different computed attractors, which satisfy the usual theoretical properties associated with attractors.

## 6. Conclusion

It has been demonstrated that attempts to compute numerical solutions of the Lorenz equations and associated statistical properties are contaminated by errors due to the use of a discrete numerical method and finite computer arithmetic. Similar behavior has been discovered for the Rössler equations (Stuart & Humphries, 1996; Rössler 2000) and a particular one-dimensional partial differential equation, the Kuramoto-Sivashinsky equation (Yao 2002). Reasons for this behavior have been advanced. They suggest that non-linear differential equations are not hyperbolic systems since they have three or more discrete singular points. Each singular point has its own stable and unstable manifolds, which may form one or more virtual separatrices. The existence of a virtual separatrix admits the possibility of a computed trajectory actually jumping through it. Such behavior violates the differential equations. Even in the presence of bounded “computed

results,” this possibility should be examined before accepting “computed results” as useful numerical approximations to the solution of the differential equations.

## References

- Abraham R. H. & Shaw C. D. 1992 “Dynamics: the geometry of behavior,” Addison-Wesley Publishing Company.
- Bowen, R. 1975 “Equilibrium states and the ergodic theory of Anosov diffeomorphism,” Vol. **470**, Lecture Notes in Mathematics, Springer-Verlag
- Dawson S., Grebogi C., Sauer T. & Yorke J. A. 1994 “Obstructions to shadowing when a Lyapunov exponent fluctuates about zero,” *Physical Review Letters*, Vol. **73**, Number 14, October 3, pp. 1927-1930.
- Do Y. & Lai Y. C. 2004 “Statistics of shadowing time in nonhyperbolic chaotic systems with unstable dimension variability,” *Physical Review E*, Vol. 69, 016213.
- Guckenheimer J. & Holmes P. 1983 “Nonlinear Oscillations, Dynamical Systems, and Bifurcations of Vector Fields,” Springer-Verlag,.
- Morales C. A., Pacifico M. J., & Pujals E. R. 2002 “Robust transitive singular sets for 3-flows are partially hyperbolic attractors or repellers,” Reprint.
- Palis J. 2000 “A global view of dynamics and a conjecture on the denseness of attractors,” *Astérisque*, Vol. **261**, pp. 335-347.
- Rössler O. E. 2000 “Chaos, hyperchaos and the double-perspective,” *The Chaos Avant-Garde: memories of the early days of chaos theory*, edited by R. Abraham and Y. Ueda, World Scientific, pp. 209-219.
- Smale S. 1998 “Mathematical problems for the next century,” *The Mathematical Intelligencer*, Vol. **20**, No. 2, pp. 7-15.
- Stuart & Humphries, 1996 “Dynamical systems and numerical analysis,” Cambridge University Press, pp. 532-533.
- Tucker W. 2002 “A rigorous ODE solver and Smale’s 14<sup>th</sup> problem,” *Foundations of Computational Mathematics*, Vol. **2** : **1**, pp. 53-117; or, <http://www.math.cornell.edu/~warwick/main/papers.html>.
- Viana Marcelo 2000 “What’s new on Lorenz strange attractors?” *The Mathematical Intelligencer*,. Vol. **22**, No. 3, pp. 6-19.
- Yao L. S. 1999 “A resonant wave theory,” *J. Fluid Mech.*, **395**, pp.237-251.

Yao L. S. 2002 “A study of a model nonlinearity,”

<http://arxiv.org/ftp/physics/papers/0506/0506169.pdf> .

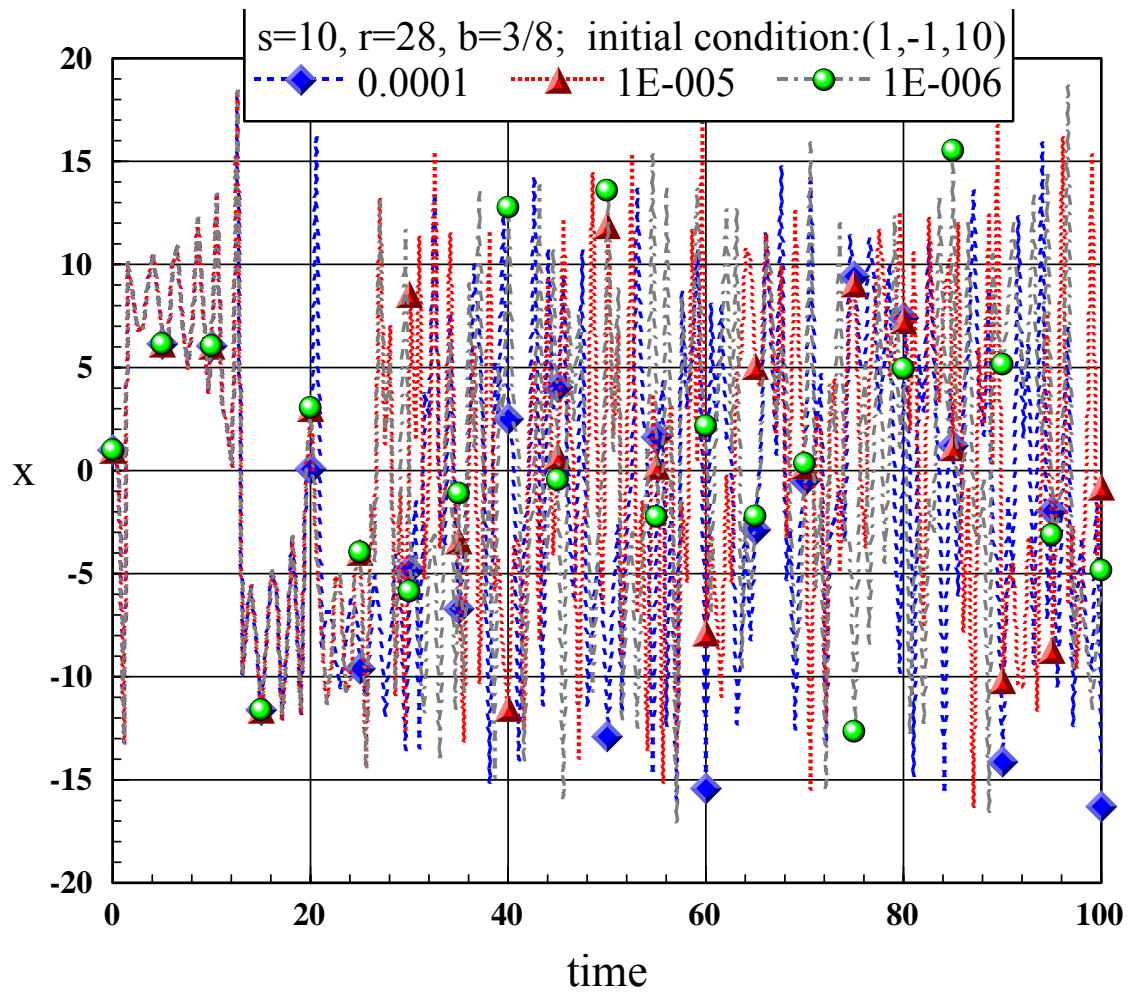


Figure 1. Plots of the time history of  $x$  for three different time-steps showing that the “computed results” for a time-step of 0.0001 start to diverge from the other two at approximately  $t=20$ . They all become different after  $t = 30$ .

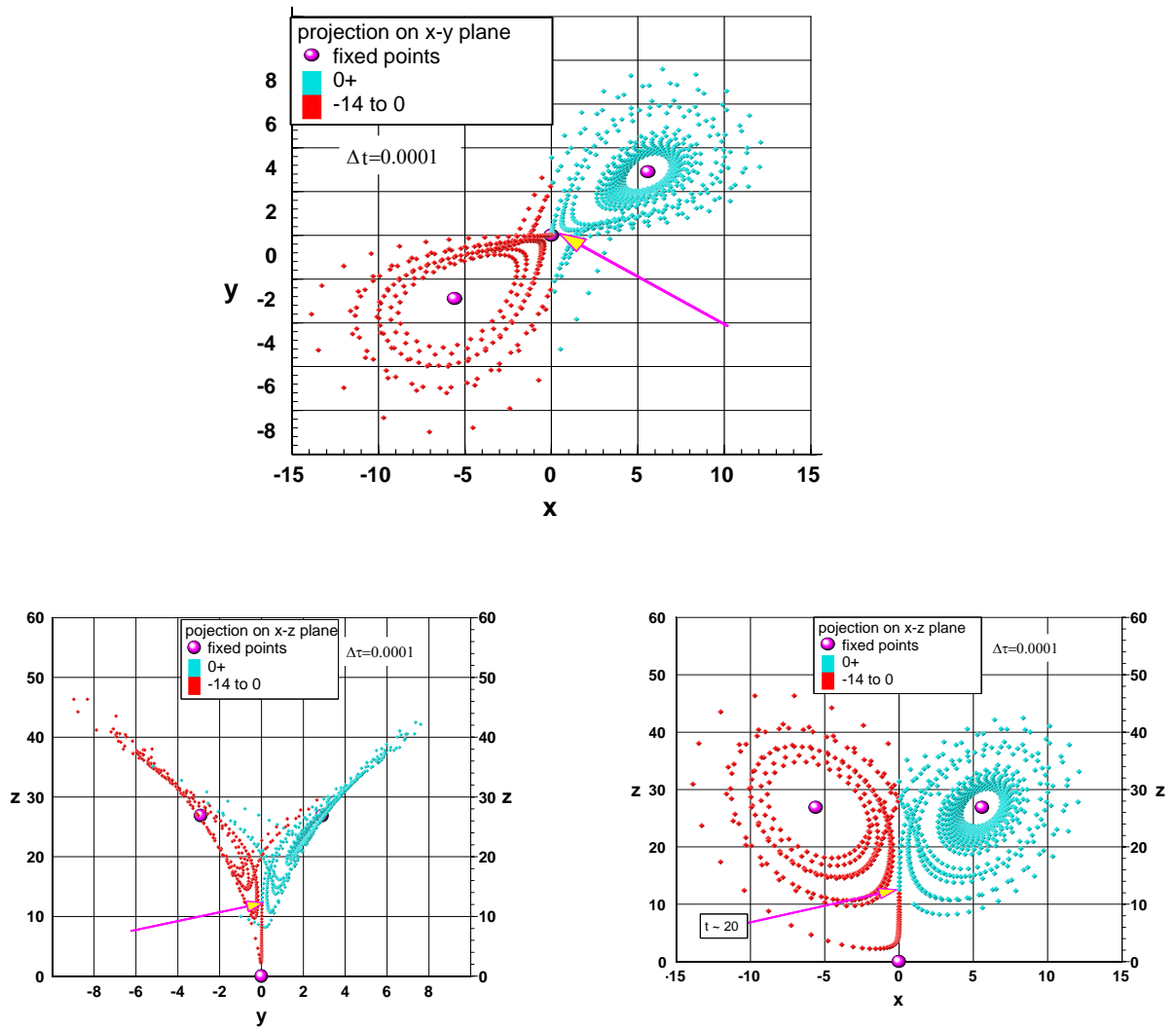


Figure 2. Plots of three projections for the first 300,000 computed points with a time-step of 0.0001. An arrow marks the location where the computed trajectory starts to deviate from those for other time-steps. This divergence occurs at time slightly smaller than 20.



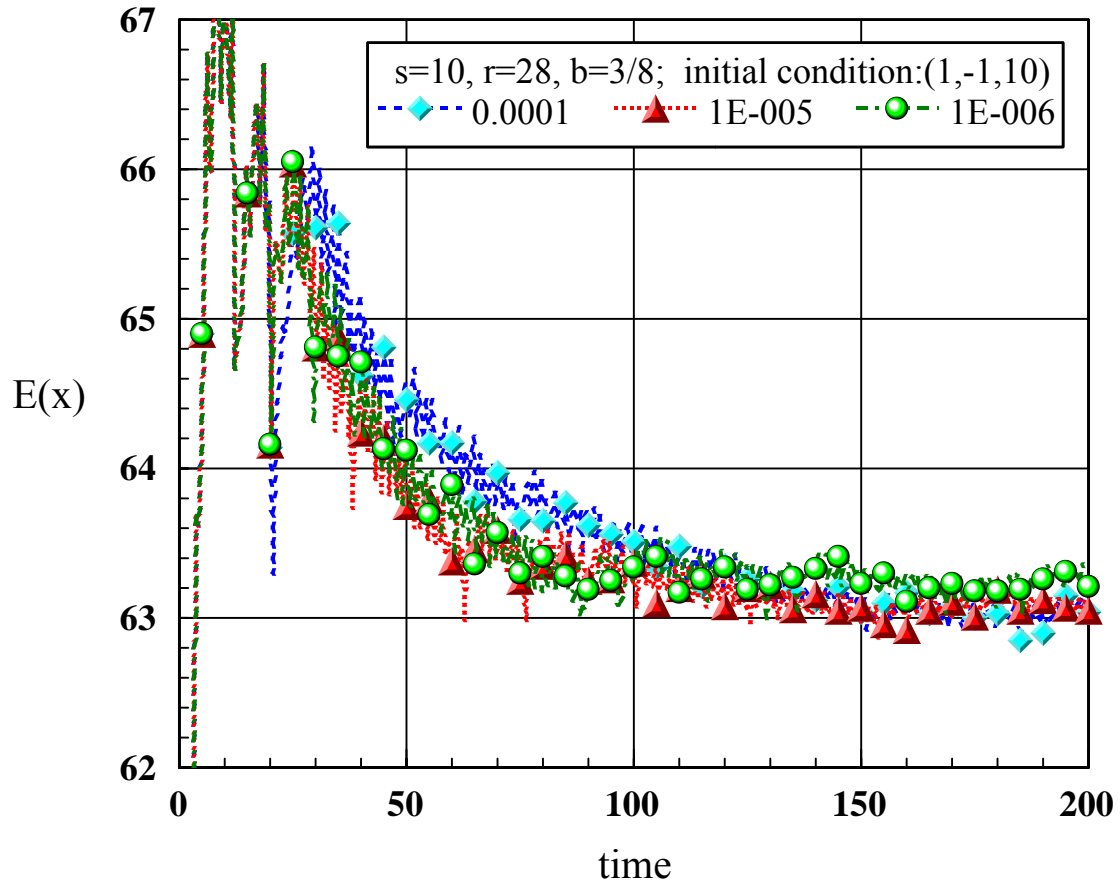


Figure 3. The autocorrelations of computed  $x(t)$  (Section 2) for three different time-steps showing that they are all different. Extending the computation to  $t=2000$  did not improve the convergence, and shows that  $E(x)$  continuously fluctuates and does not show any tendency to approach a constant.

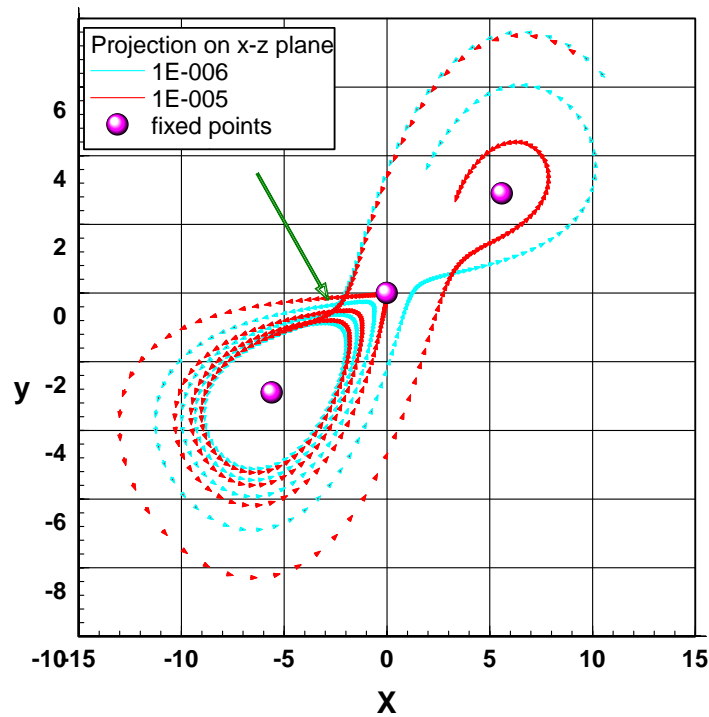


Figure 4a. “Computed results” for two different time-steps with identical initial conditions showing the exponential growth of the numerical errors. The arrow marks the starting location of dramatic error amplification.

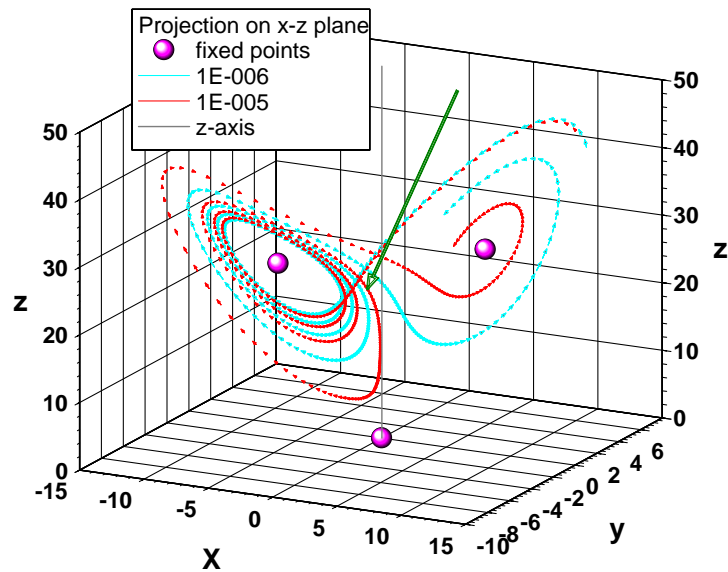


Figure 4b. A three-dimensional view of Figure 4a.

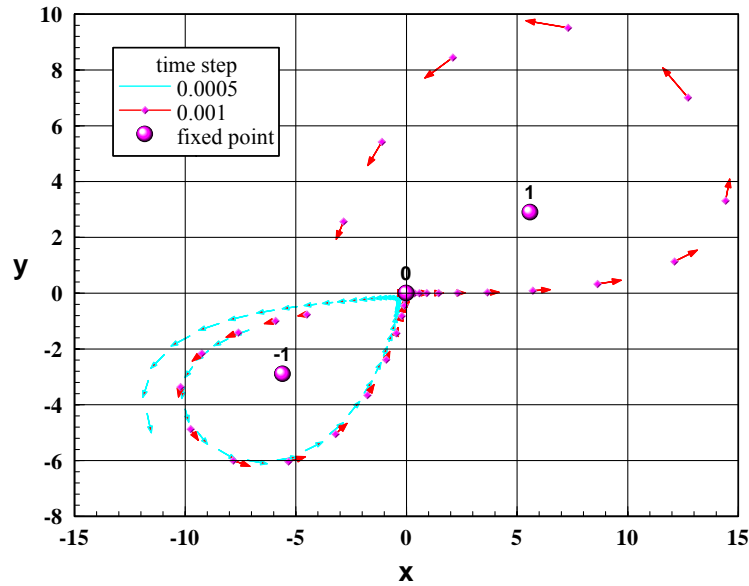


Figure 5a. “Computed results” for two different time-steps with identical initial conditions showing dramatic growth of the numerical errors. The trajectory associated with time-step of 0.001 jumps through the virtual separatrix.

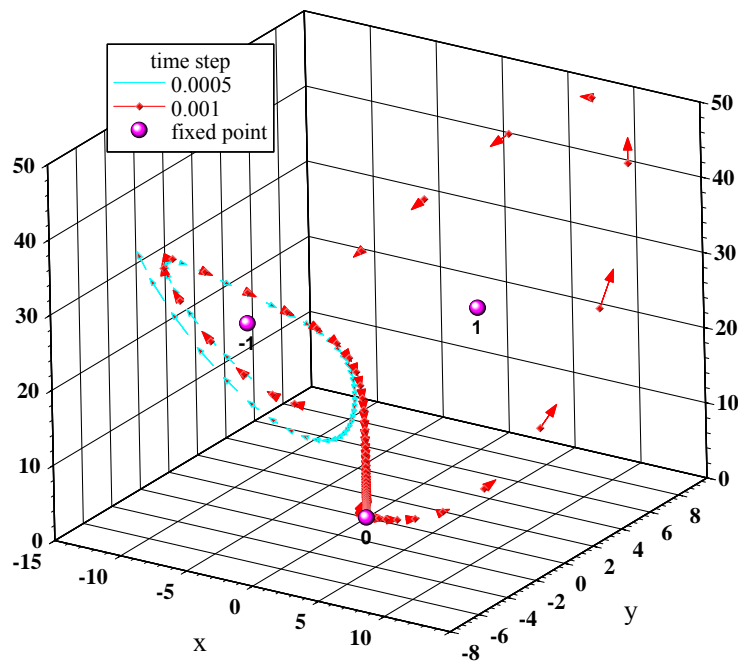


Figure 5b. A three-dimensional view of Figure 5a.

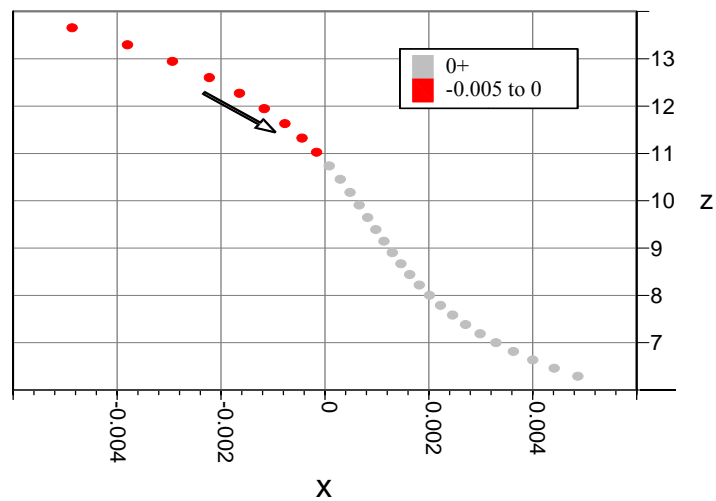
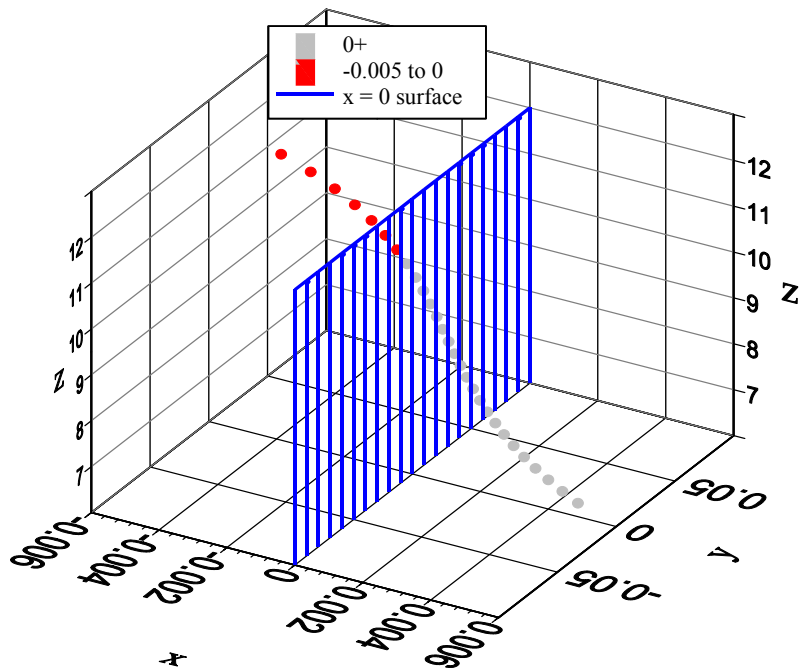


Figure 5c. Amplified views of Figure 5a & 5b.

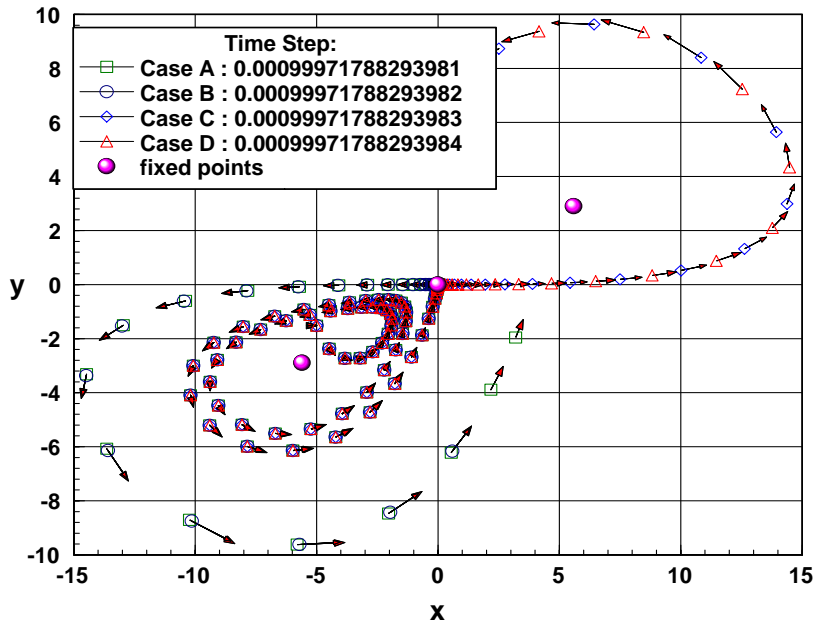


Figure 6a. “Computed results” showing that a dramatic growth of numerical errors occurs with time-steps of extremely small differences. Two of the computed trajectories jump through the virtual separatrix.

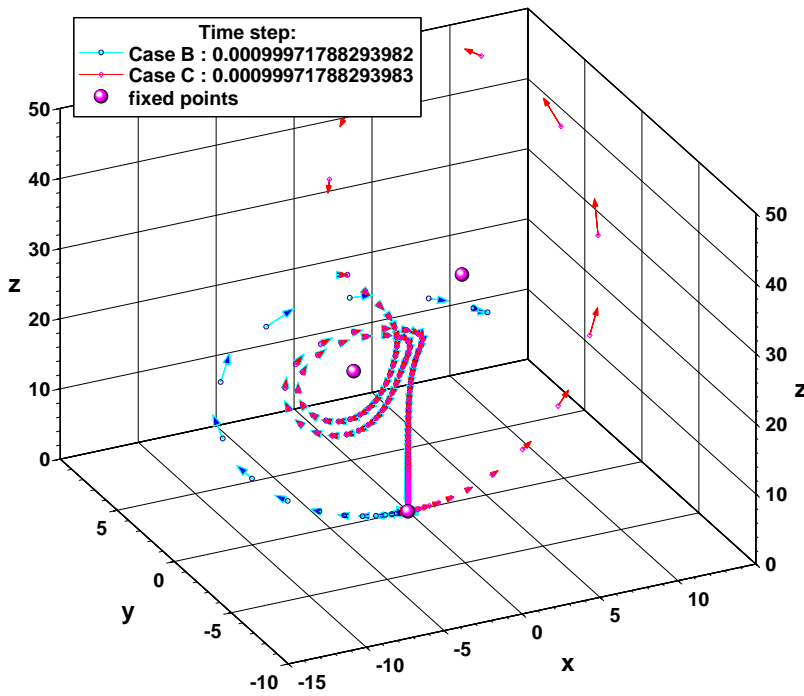


Figure 6b. A three-dimensional view of Figure 6a.

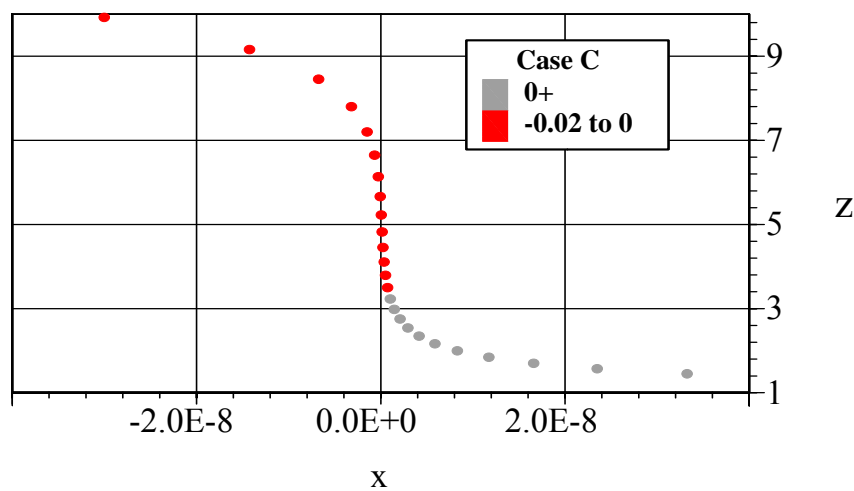
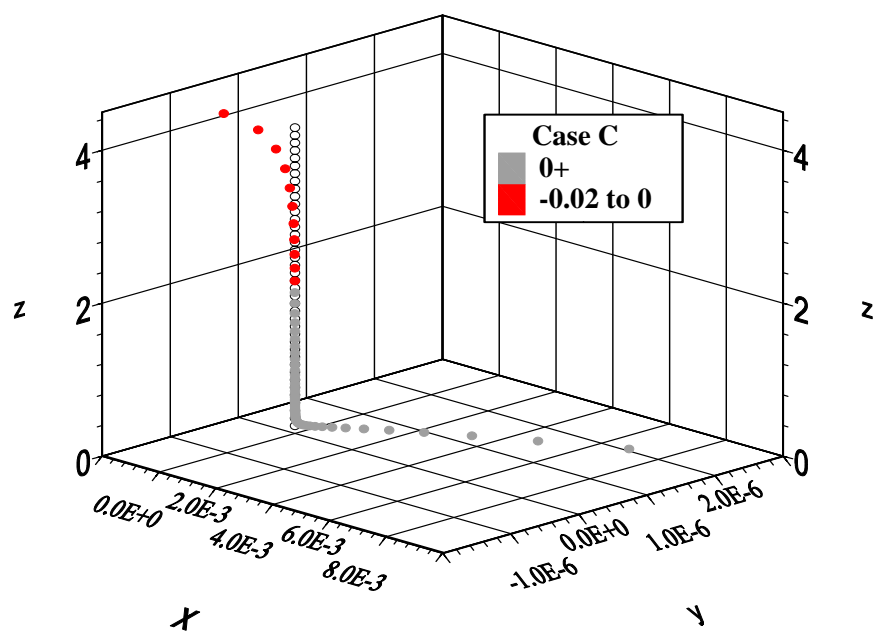


Figure 6c. Amplified views of Figure 6a & 6b.

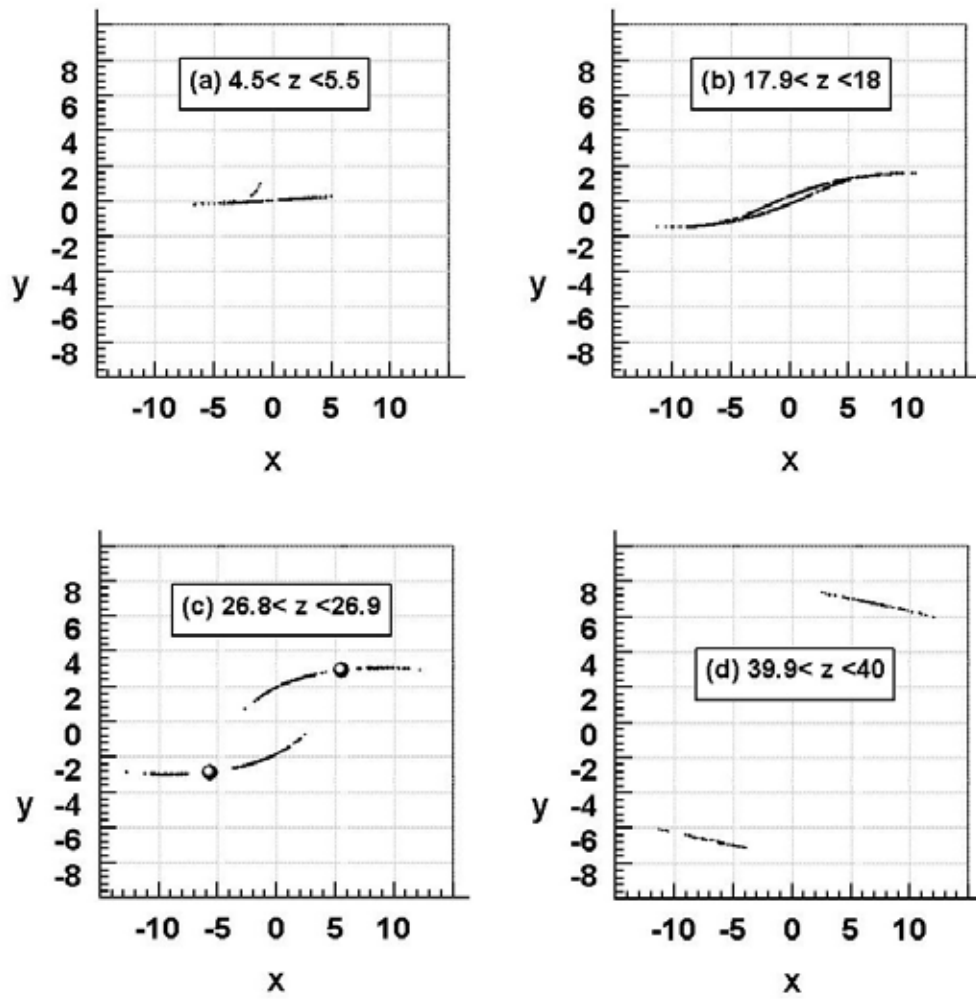


Figure 7. Cross-sections of a computed Lorenz attractor at selected  $z$  locations showing that its thickness is thin and that its point density is not uniform.

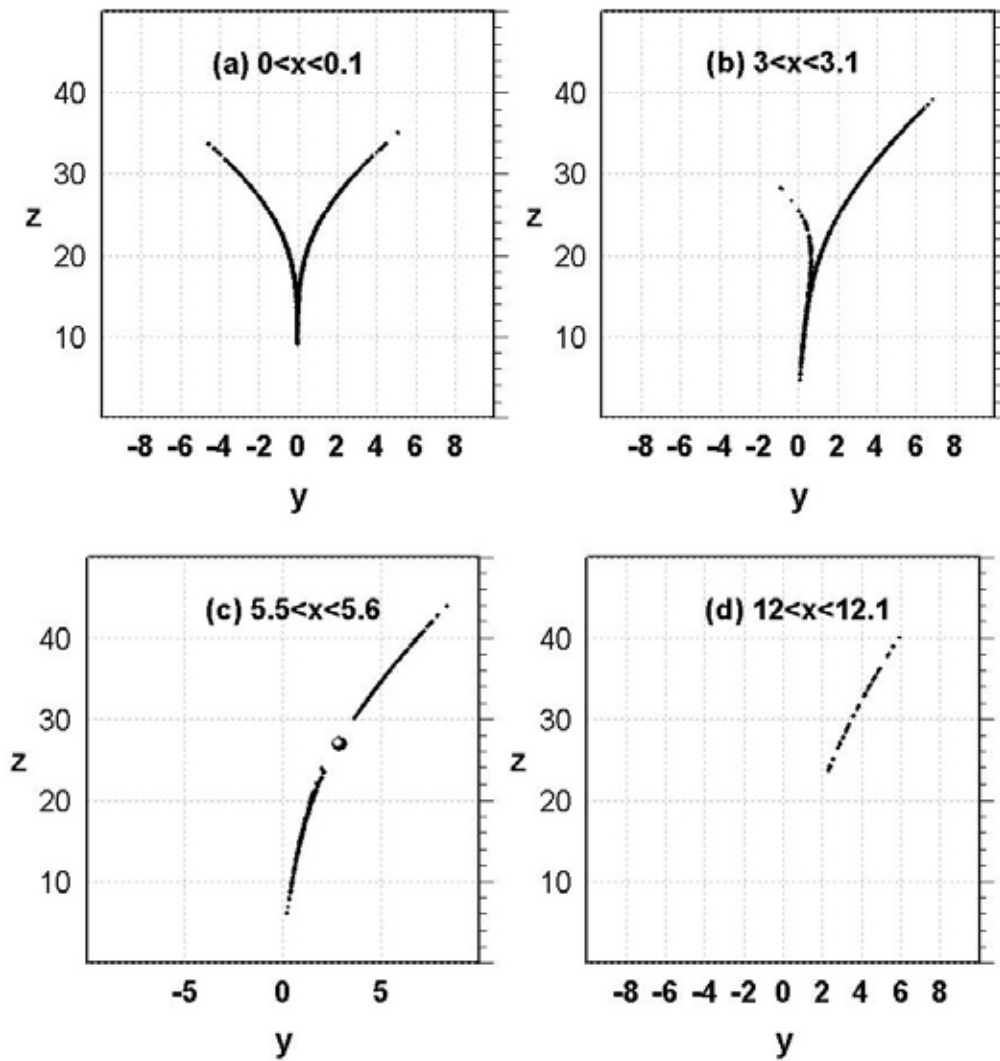


Figure 8. Cross-sections of a computed Lorenz attractor at selected  $x$  locations showing that its thickness is thin and that its point density is not uniform.



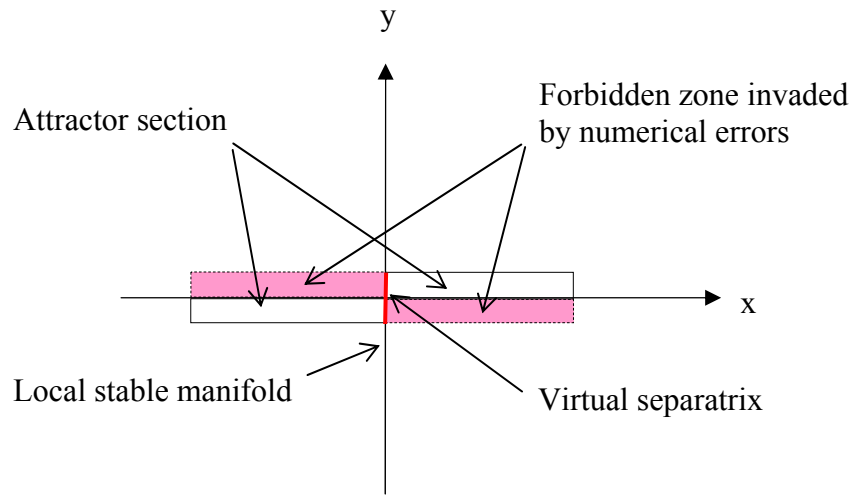


Figure 9. Enlarged cartoon of Figure 7a after mapping the local unstable manifold to the  $x$ -axis. The local stable manifold inside the attractor forms a finite virtual separatrix whose height is about  $0 \leq z \leq 15$  (see equations 5 & 7).